# Supporting information

# Construct an "Immunogenic Cell Death" Amplifier based on Fe-MOFs by accelerating Fe(III) reduction strategy for Integration of Tumor Diagnosis, Treatment, and Prevention

**Kexin Luo‡[a], Sasha You‡[a], Jingyu Chen‡[b], Bin Chi‡[c], Kai Zhang[d], Jian Tian[a], Xiyue Feng[a], Wang Ye[a], Yingxi Wang[a], Ling Li*[a], Xiaolan Yu*[b], Jing Wang*[c]**

a. Hubei Key Laboratory for Precision Synthesis of Small Molecule Pharm aceuticals & Ministry of Education Key Laboratory for the Synthesis and Appli cation of Organic Functional Molecules & Collaborative Innovation Center for Advanced Organic Chemical Materials Co-constructed by the Province and Min istry, Hubei University, Wuhan 430062, P. R. China.

b. State Key Laboratory of Biocatalysis and Enzyme Engineering, Hubei C ollaborative Innovation Center for Green Transformation of Bio-resources, Hube i Key Laboratory of Industrial Biotechnology School of Life Sciences, Hubei University, Wuhan, 430062, China.

c. Department of Radiology, Union Hospital, Tongji Medical College, Hua zhong University of Science and Technology, Wuhan 430022, China.

d. College of Chemistry and Chemical Engineering, Huanggang Normal U niversity, Huanggang, 438000, China.

* Corresponding author.
Email address: lingli@hubu.edu.cn(L. Li)

## Experimental

### Chemicals and reagents

iron chloride hexahydrate ($FeCl_3 \cdot 6H_2O$, 99%), copper nitrate hexahydrate ( $Cu(NO_3) \cdot 3H_2O$, 99.%), 2-aminoterephthalic acid(2-$NH_2$-BDC), molybdenyl acetyl acetonate,methotrexate(MTX),glutathione(GSH),3,3',5,5'-tetramethylbenzidine(TMB) were obtained from Macklin, Shanghai, China. Hydrogen peroxide ($H_2O_2$), N, N-dimethylformamide (DMF, 99.5%), Hydrochloric acid (HCl, 36%~38%), and ethanol ($C_2H_5OH$, 95%) were purchased from Sinopharm Group Chemical Reag ent. Sodium carbonate($Na_2CO_3$, 99.5%), Polyvinylpyrrolidone(PVP) were from A laddin Industrial Company. CCK-8 assay, DCFH-DA, Annexin V-AbFlour$^{TM}$ 48 8/PI were purchased from Abbkine, DAPI was purchased from solarbio, PBS, DMEM were purchased from Servicebio, Calreticulin Rabbit Monocional Antibo dy were purchased from Beyotime, Fresh deionized water was used for all exp eriments. All these reagents were not further purified and used as received.

### Materials characterization

Transmission electron microscope (TEM) images were obtained by a G②2 0S-TWIN transmission electron microscope (USAFEI), Scanning electron micros cope (SEM) images were obtained by a JSM6510LV scanning electron microsc ope (JEOL, Japan), Field emission scanning electron microscope(FESEM) imag es were obtained by a SIGMA500 field emission scanning electron microscope (Beijing Opton Optical Technology Co, Ltd, China) respectively. The powder X-ray diffraction (XRD) was performed using an X-ray diffractometer powder diffractometer (Bruker D8, Bruker Company, USA). Fourier transform infrared spectra (FTIR, PerkinElmer, USA) were sensed in the region from 400 to 4000 cm−1 by means of the KBr pressed disk technique at room temperature. X-ray photoelectron spectroscopy (XPS) was obtained on a photoelectron spectrometer

(ESCALAB 250Xi X-ray, Thermo Fisher Scientific Inc., Waltham, MA, USA) with the monochromatic Al Ka source. Dynamic light scattering (DLS, HGY15, Zetasizer Nano ZS90Zetasizer Nano ZS90, Malvern, UK) was used to determin e the particle size distribution and the zeta potential of the Cu/Fe-$NH_2$-MIL-10 1@$MoO_2$/MTX Nanoparticles. Inductively coupled plasma optical emission Spe ctrometry (ICP-OES optimal8000, PE, UK).

**Detection of •OH in vitro**

To investigate the catalytic performance of the materials, their hydroxyl rad ical (•OH) generation capability was evaluated using 3,3',5,5'-tetramethylbenzidin e (TMB) as a probe. TMB can be oxidized by •OH to form oxidized TMB (o x-TMB), exhibiting a characteristic absorption peak at 652 nm. Fe-$NH_2$-MIL-10 1, Cu/Fe-$NH_2$-MIL-101, and Cu/Fe-$NH_2$-MIL-101@$MoO_2$ were individually disp ersed in phosphate-buffered saline (PBS, pH 5.8) containing $H_2O_2$ (10 mM) an d TMB (50 μg/mL). After incubation for 5 mins or 1 h, the absorbance chang es at 652 nm were measured using a UV-vis spectrophotometer.

**Photo-thermal efficiency of Cu/Fe-$NH_2$-MIL-101@$MoO_2$**

The photothermal conversion efficiency (η) of Cu/Fe-$NH_2$-MIL-101@$MoO_2$ can be calculated according to the equation.

$$\eta = \frac{\mathrm{hs}(T_{\max} - T_{surr}) - Q_{dis}}{I(1-10^{-A_{808}})} \qquad (1)$$

The $T_{max}$ (K) represents the highest equilibrium temperature; $T_{surr}$ (K) is th e environment temperature. The $Q_{dis}$ (W) represents heat loss due to absorption of light by the container, and it is calculated to be equal to 0 mW. I (W) is i ncident laser power. $A_{808}$ is the absorbance of samples at 808 nm. Where h ( W $cm^{-2}$ $K^{-1}$) is heat transfer coefficient, S ($cm^2$) is the surface area of the con tainer.

$$\tau_s = \frac{m_D c_D}{hs} \qquad (2)$$

$$t = -\tau_s \ln\theta \qquad (3)$$

$$\theta = \frac{T_{RT} - T_{sur}}{T_{max} - T_{sur}} \qquad (4)$$

The $\tau_s$ means the sample system time constant, $m_D$ and $c_D$ are the mass a nd heat capacity of the solvent.

**Study of Michaelis-Menten kinetics**

The POD-like activity of the Cu/Fe-$NH_2$-MIL-101@$MoO_2$ and Cu/Fe-$NH_2$-MIL-101@$MoO_2$+NIR were studied in a phosphate buffer solution (10 mM, pH 5.8, 5 mL) containing Cu/Fe-$NH_2$-MIL-101@$MoO_2$(0.1 mg/mL) and various con centrations of $H_2O_2$ (0−10 mM). For each group experiment, the absorbance of ox-TMB at 652 nm was documented every 5 min at room temperature.

$$v = \frac{v_{max}[s]}{k_m + [s]} \qquad (1)$$

$$\frac{1}{v} = \frac{k_m}{v_{max}} \cdot \frac{1}{s} + \frac{1}{v_{max}} \qquad (2)$$

The rates were plotted against the substrate content and then fitted with th e Michaelis-Menten curves (equation 1). Furthermore, a linear double-reciprocal plot (Lineweaver-Burk plot, equation 2) was used for determining the $K_m$ and $V_{max}$ ([S] is the substrate concent).

GPx-like activity of Cu/Fe-$NH_2$-MIL-101@$MoO_2$ and Cu/Fe-$NH_2$-MIL-101@ $MoO_2$+NIR was carried out by measuring the change of absorbance. The Cu/F e-$NH_2$-MIL-101@$MoO_2$ was implemented in a phosphate buffer solution (10 m M, pH 5.8, 5 mL) containing Cu/Fe-$NH_2$-MIL-101@$MoO_2$ (0.1 mg/mL) and va rious concentrations of GSH (0.5−10 mM) and DTNB(0.1 mg/mL). For each g roup experiment, the absorbance of DTNB at 412 nm was documented every 5 min at room temperature.

**Drug loading and release**

10 mg of Cu/Fe-$NH_2$-MIL-101 and Cu/Fe-$NH_2$-MIL-101@$MoO_2$ were respe ctively added into a culture flask with 10 mL Methotrexate Solution (0.1g/L). After being placed at room temperature and without light for 24 h, 48 h and 72 h, a UV-vis spectrophotometer was used to determine the concentration of r esidual MTX at the calibrated maximum wavelength of 306 nm. The drug load ing can be calculated according to the following Equation:

$$\text{Drug loading} = V(C_{\text{initial drug}} - C_{\text{drug in supernatant}})$$

According to the above method, drug loading of Cu/Fe-$NH_2$-MIL-101 and Cu/Fe-$NH_2$-MIL-101@$MoO_2$ can be analyzed. The MTX-loaded Cu/Fe-$NH_2$-MIL -101 and Cu/Fe-$NH_2$-MIL-101@$MoO_2$ particles were respectively placed into a dialysis bag (Cat No: MD10, MWCO:14000D, Nominal Flat Width:10mm) and then immersed in 10 mL of PBS solution at different values of pH (pH=7.4 o r 5.8), different GSH concentration(GSH=2mM or 10mM) and at a temperature of 37 ℃. At different points in time, the drug release medium (3 mL) was wi thdrawn for analysis by UV-Vis absorption spectroscopy at a wavelength of 30 6nm.The drug release concentration is calculated by correlating UV absorption values with the drug's standard curve.

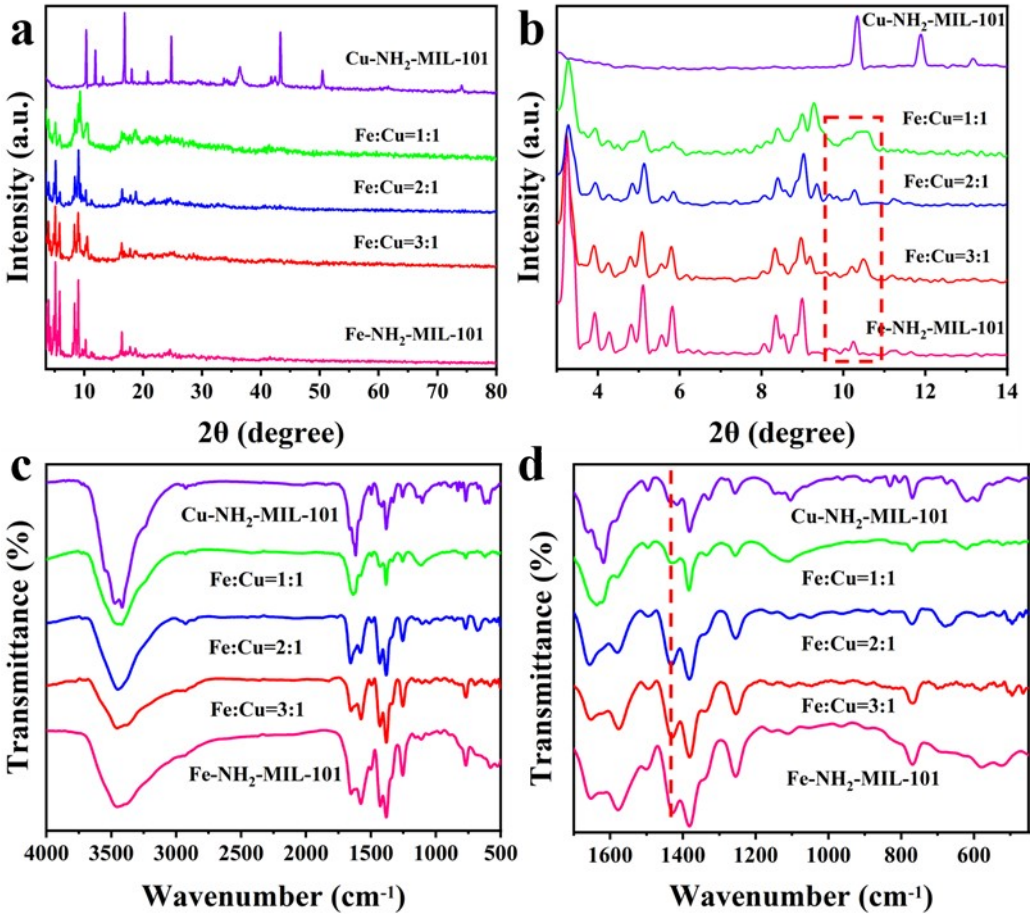


Figure S1. (a, b) XRD of Cu-$NH_2$-MIL-101, Fe-$NH_2$-MIL-101 and Cu/Fe-$NH_2$-MIL-101. (c, d) FT-IR of Cu-$NH_2$-MIL-101, Fe-$NH_2$-MIL-101 and Cu/Fe-$NH_2$-MIL-101.

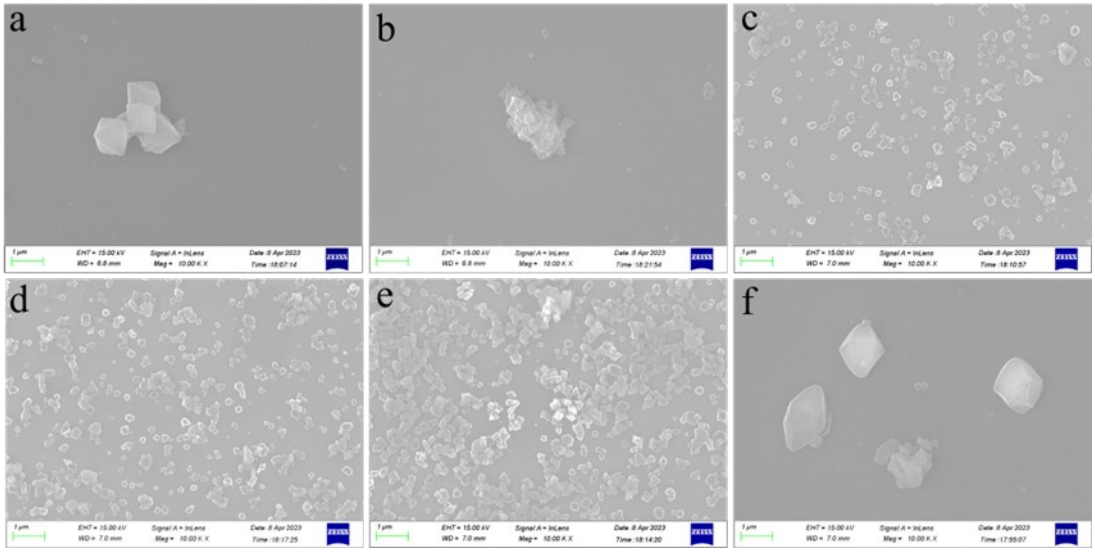


Figure S2. SEM image of (a)Fe-$NH_2$-MIL-101, (b)Cu/Fe-$NH_2$-MIL-101-1, (c)Cu/Fe-$NH_2$-MIL-101-2, (d)Cu/Fe-$NH_2$-MIL-101-2, (e)Cu/Fe-$NH_2$-MIL-101-3 and (f)Cu-$NH_2$-MIL-101

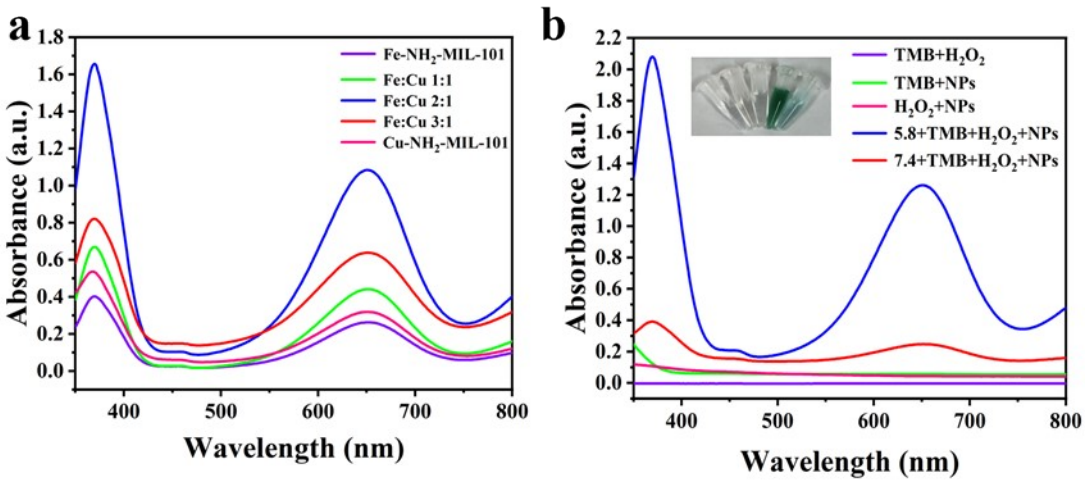


Figure S3. (a)TMB color development experiment for different materials. (b)TMB color development experiments under different pH conditions.

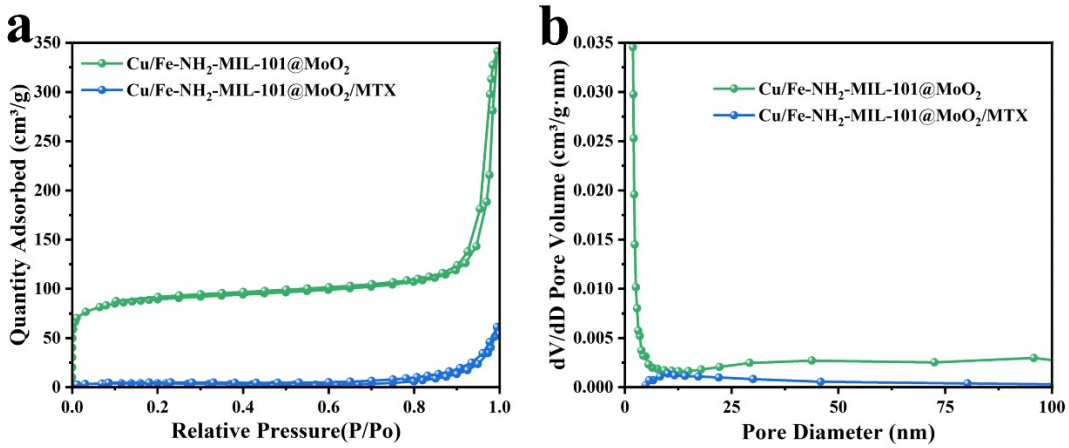


Figure S4. (a)Nitrogen ($N_2$) adsorption desorption curves of the Cu/Fe-$NH_2$-MIL-101@$MoO_2$ and Cu/Fe-$NH_2$-MIL-101@$MoO_2$/MTX. (b)Pore size distribution of Cu/Fe-$NH_2$-MIL-101@$MoO_2$ and Cu/Fe-$NH_2$-MIL-101@$MoO_2$/MTX.

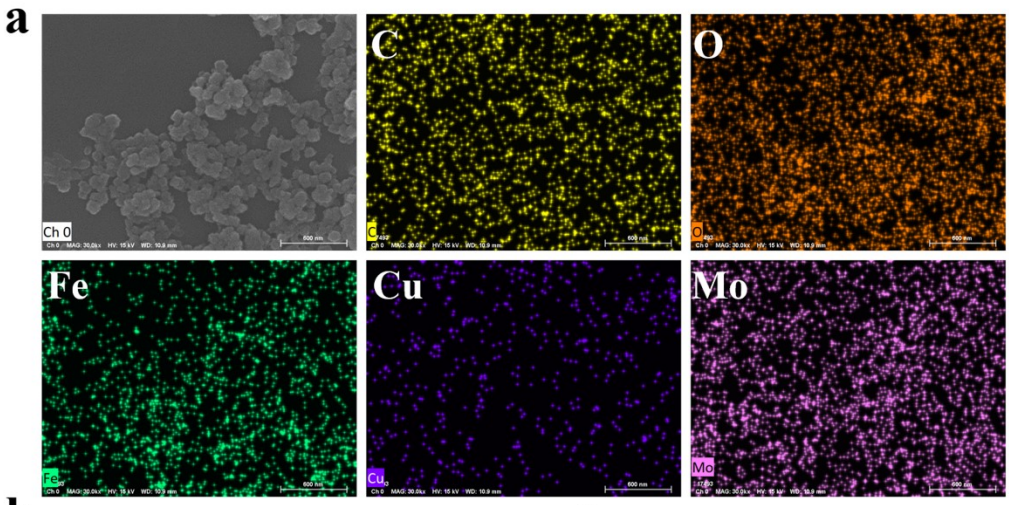


b

| Total Spectrum of Distribution Plots | | | | | | |
|---|---|---|---|---|---|---|
| Element | Signal type | abs.error[%] (1 sigma) | abs.error[%] (3 sigma) | Wt% | rel.error[%] (3 sigma) | At% |
| C | EDS | 0.53 | 1.59 | 35.34 | 73.10 | 55.15 |
| O | EDS | 0.43 | 1.30 | 28.21 | 74.69 | 33.05 |
| Fe | EDS | 0.12 | 0.36 | 31.55 | 18.51 | 10.59 |
| Cu | EDS | 0.05 | 0.16 | 2.60 | 102.11 | 0.77 |
| Mo | EDS | 0.04 | 0.12 | 2.30 | 83.53 | 0.45 |
| Total | | | | 100.00 | | 100.00 |

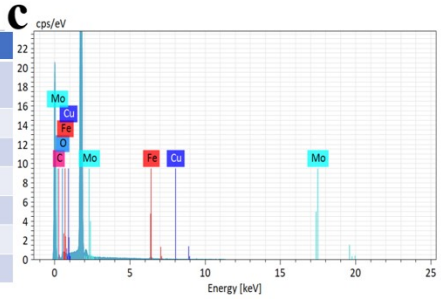


Figure S5. (a)Mapping image of Cu/Fe-$NH_2$-MIL-101@$MoO_2$. (b, c) EDX of Cu/Fe-$NH_2$-MIL-101@$MoO_2$.

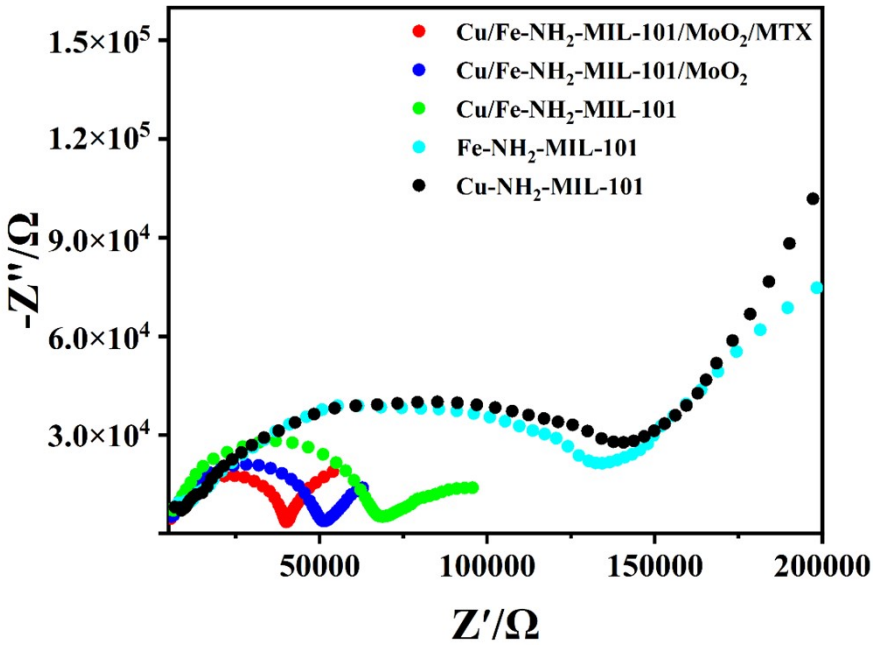


Figure S6. Impedance diagrams of Cu-$NH_2$-MIL-101, Fe-$NH_2$-MIL-101, Cu/Fe-$NH_2$-MIL-101, Cu/Fe-$NH_2$-MIL-101@$MoO_2$, Cu/Fe-$NH_2$-MIL-101@$MoO_2$/MTX

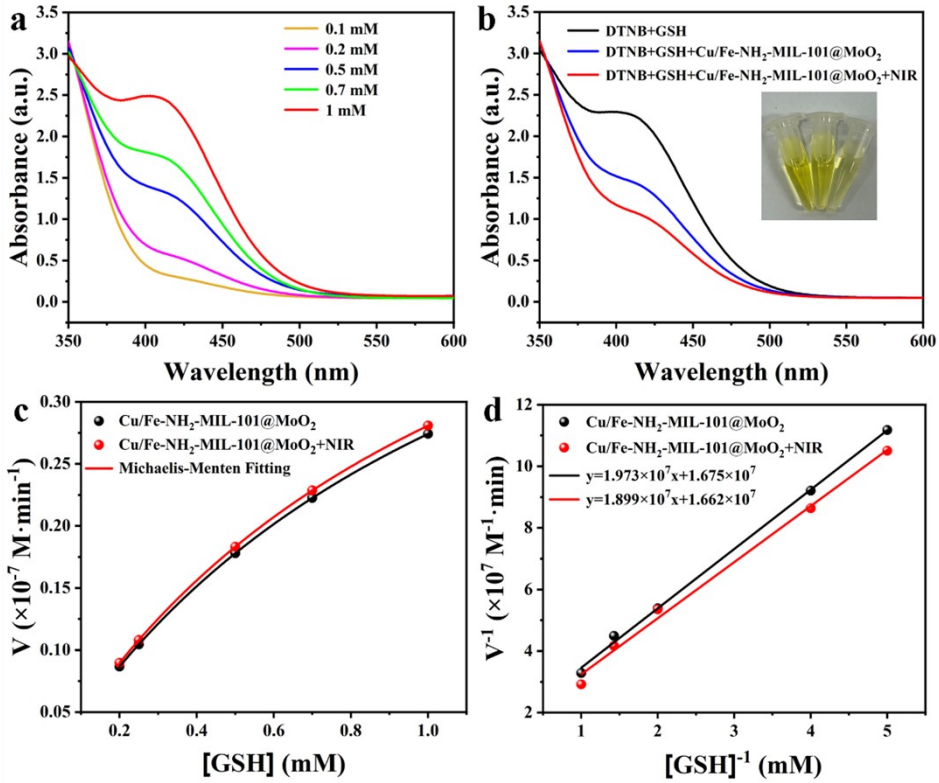


Figure S7. (a)The color experiment of DTNB probe at different GSH concentra tions. (b)The color experiment of DTNB probe with Cu/Fe-$NH_2$-MIL-101@Mo $O_2$ or Cu/Fe-$NH_2$-MIL-101@$MoO_2$+NIR. (c)Michaelis-Menten kinetic analysis of GSH concentrations catalyzed by Cu/Fe-$NH_2$-MIL-101@$MoO_2$ or Cu/Fe-$NH_2$-MI L-101@$MoO_2$+NIR.(d) Lineweaver-Burk plots of GSH concentrations catalyzed by Cu/Fe-$NH_2$-MIL-101@$MoO_2$ or Cu/Fe-$NH_2$-MIL-101@$MoO_2$+NIR.

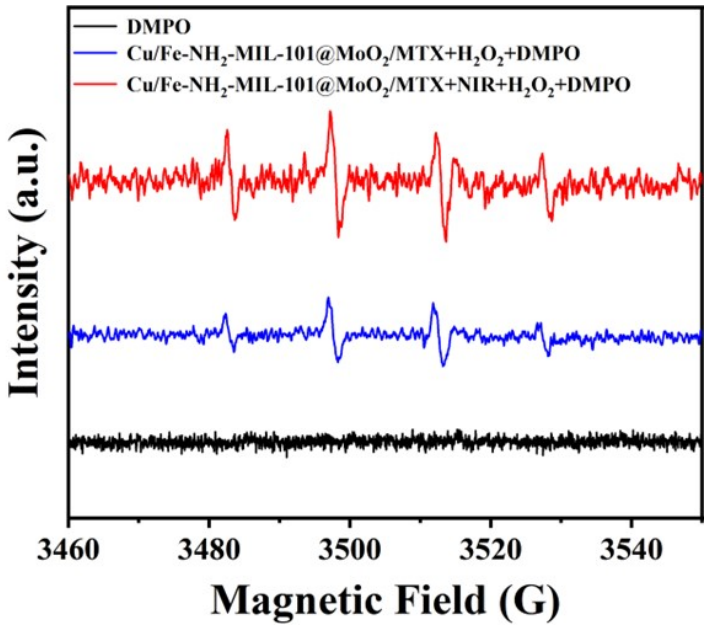


Figure S8. EPR spectra of the material

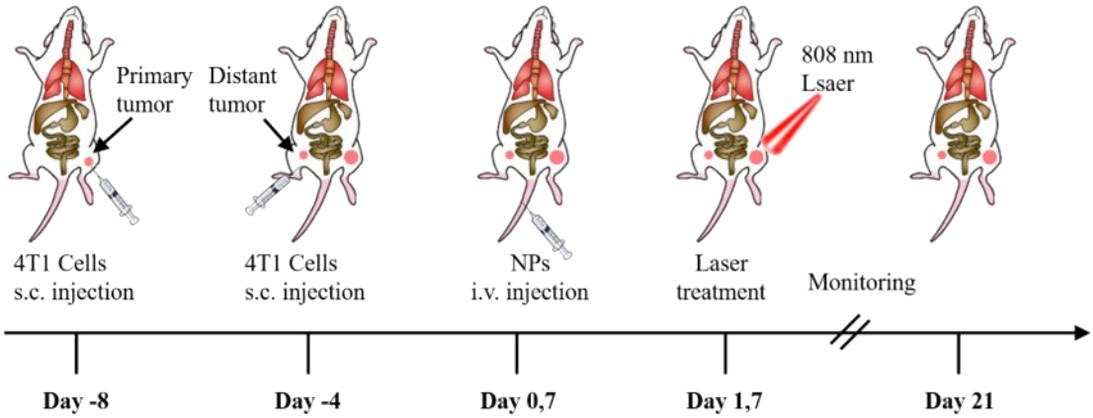


Figure S9. 4T1 tumor-bearing mice treatment process diagram

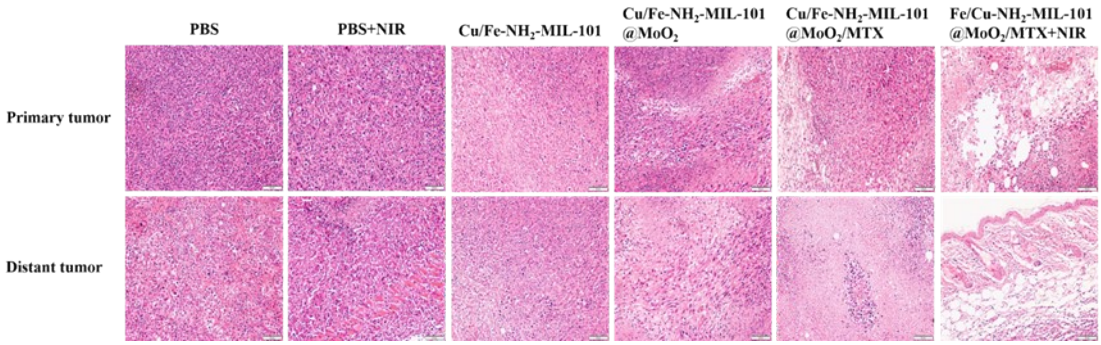


Figure S10. H&E-stained images of tumor slices obtained from different groups of mice and the scale bar is 50 μm.

Table.S1 Steady-state kinetic parameters of POD-like enzymes under NIR(on) and NIR(off) conditions

| | Km (mM) | Vm ($10^{-9}$ $M^{-1}$ • S) |
|---|---|---|
| Fe-$NH_2$-MIL-101 | 1.76 | 4.87 |
| Fe-$NH_2$-MIL-101+NIR | 1.68 | 4.88 |
| Cu/Fe-$NH_2$-MIL-101@$MoO_2$ | 1.03 | 5.85 |
| Cu/Fe-$NH_2$-MIL-101@$MoO_2$ +NIR | 0.55 | 6.00 |